Exploring the use of compound-specific carbon isotopes as a palaeoproductivity proxy off the coast of Adélie Land, East Antarctica

Kate Ashley[1], Xavier Crosta[2], Johan Etourneau[2,3], Philippine Campagne[2,4], Harry Gilchrist[1], Uthmaan Ibraheem[1], Sarah Greene[1], Sabine Schmidt[2], Yvette Eley[1], Guillaume Massé[4,5] and James Bendle[1]

[1]School of Geography, Earth and Environmental Sciences, University of Birmingham, Edgbaston, Birmingham, B15 2TT, UK
[2]EPOC, UMR-CNRS 5805, Université de Bordeaux, 33615 Pessac, France
[3]EPHE/PSL Research University, 75014 Paris, France
[4]LOCEAN, UMR CNRS/UPCM/IRD/MNHN 7159, Université Pierre et Marie Curie, 4 Place Jussieu, 75252 Paris, France
[5]TAKUVIK, UMI 3376 UL/CNRS, Université Laval, 1045 avenue de la Médecine, Quebec City, Quebec, Canada G1V 0A6

Correspondence to: James Bendle (j.bendle@bham.ac.uk)

Abstract

The Antarctic coastal zone is an area of high primary productivity, particularly within coastal polynyas where large phytoplankton blooms and drawdown of CO_2 occur. Reconstruction of historical primary productivity changes, and the associated driving factors, could provide baseline insights on the role of these areas as sinks for atmospheric CO_2, especially in the context of projected changes in coastal Antarctic sea ice. Here we investigate the potential for using carbon isotopes ($\delta^{13}C$) of fatty acids in marine sediments as a proxy for primary productivity. We use a highly resolved sediment core from off the coast of Adélie Land spanning the last ~400 years and monitor changes in the concentrations and $\delta^{13}C$ of fatty acids along with other proxy data from the same core. We discuss the different possible drivers of their variability and argue that C_{24} fatty acid $\delta^{13}C$ predominantly reflects phytoplankton productivity in open water environments, while C_{18} fatty acid $\delta^{13}C$ reflects productivity in the marginal ice zone. These new proxies have implications for better understanding carbon cycle dynamics in the Antarctica coastal zone in future paleoclimate studies.

1 Introduction

Antarctic coastal zones are important players in the global carbon cycle. The deep ocean is ventilated in these regions as part of the Southern Ocean overturning circulation, allowing waters rich in nutrients and CO_2 to be upwelled to the surface. In the absence of biological activity, most of the CO_2 would be leaked to the atmosphere. However, coastal polynyas within the Antarctic margin are areas of very high primary productivity during the spring and summer months (e.g. Arrigo et al., 2008) that rapidly reduces CO_2 to low levels through photosynthesis (Arrigo and van Dijken, 2003; Arrigo et al., 2008), resulting in surface water CO_2 undersaturation with respect to atmospheric CO_2 (Tortell et al., 2011). The subsequent export and burial of the organic carbon produced during these intense phytoplankton blooms can significantly lower atmospheric CO_2 concentrations (Sigman and Boyle, 2000). Therefore, any change in the consumption of these nutrients by

phytoplankton, or any change in phytoplankton community structure, may affect the air-sea CO_2 exchange in this region.

Records of past phytoplankton productivity offer an opportunity to document the drivers of primary productivity at different timescales from pluri-decadal to millennial. In the Antarctic coastal zone past work has focused on records of organic carbon, biogenic silica and diatom abundances (Leccaroni et al., 1998; Frignani et al., 1998; Denis et al., 2009; Peck et al., 2015). These proxies however may provide a biased view of phytoplankton productivity as they only record a signal of siliceous productivity and may suffer from alteration during settling and burial (Beucher et al., 2004; Tréguer et al., 2017). As such, there is no robust understanding of how such records respond to surface water CO_2 which is of major importance in the context of Antarctic coastal sea ice changes.

Here we investigate the use of compound specific carbon isotope analysis ($\delta^{13}C$) of freely extractable (using a standard solvent extraction protocol), saturated algal fatty acids (FAs) in marine sediments as a potential integrative proxy for reconstructing primary productivity in a polynya environment. Fatty acids have the potential to be a useful palaeoproductivity tool in this region due to their ubiquitous presence within marine sediments, while other commonly used compounds, such as alkenones, are absent, Fatty acids are also able to persist within the sediments for several thousand years, meaning they have the potential to be applied over long time spans in contrast to more labile compounds such as highly branches isoprenoid alkenes (HBIs). Furthermore, fatty acids are amenable to isotope analysis allowing them to yield more detailed information about the environment.

Previous studies in the highly-productive regions of the Southern Ocean have highlighted the potential for using compound-specific isotopes from algal biomarkers in sediments to track primary productivity changes both spatially and temporally. Villinski et al. (2008) found that the spatial variation in pCO_2 in the Ross Sea was associated with a variation in the $\delta^{13}C$ of sedimentary organic carbon and sterol biomarkers, most likely due to a change in isotopic fractionation associated with the photosynthetic drawdown of CO_2. Their results demonstrate that the spatial variation in surface water CO_2 is recorded in sedimentary organic matter and algal biomarkers. We explore this further as well as looking into other potential drivers of compound-specific carbon isotopes.

We use samples from core DTGC2011, a 4.69 m sediment core recovered from offshore Adélie Land, East Antarctica, spanning the last ~400 years. The core chronology is based on radiocarbon dates and confirmed by ^{210}Pb excess activity measurements, which indicate that DTGC2011 spans the 1580-2000 C.E. period with a mean sedimentation rate of ~1 cm yr^{-1} (Supplementary Information S1). In order to understand the signal recorded by the FAs, we estimate the most likely biological source of these compounds and the habitat and season of production. Moreover, we compare downcore changes in FA concentrations and $\delta^{13}C$ with other proxy data from the same core.

Environmental setting

The Adélie drift is located in the Dumont D'Urville Trough in the Adélie Basin, ca. 35 km offshore from Adélie Land (Fig. 1). This is a 1000 m deep, glacially scoured depression on the East Antarctic continental shelf,

78 bounded to the east by the Adélie Bank. Sea ice plays a key role on the dynamics of the region, with both fast

79 ice and pack ice present off the coast of Adélie Land. A large bank of fast ice forms annually between 135 and

80 142°E, and extends up to 120 km away from the coast (Massom et al., 2009). On the north edge of this fast ice

81 buttress is an inlet of open water forming a polynya, an area of open water surrounded by sea ice (Bindoff et al.,

82 2000).

83 The Adélie Coast is characterized by extremely high primary productivity, with phytoplankton assemblages

84 dominated by diatoms (Beans et al., 2008). The site itself is located close to the Dumont D'Urville polynya

85 (DDUP), with an annual net primary productivity (NPP) of 30.3 g C m^{-2} a^{-1}, but is also directly downwind and

86 downcurrent of the much larger and highly productive Mertz Glacier polynya (MGP) to the east, with an annual

87 NPP of 39.9 g C m^{-2} a^{-1} (Arrigo et al., 2015). Various factors are known to drive productivity trends in the

88 Southern Ocean, including open water area, glacial melt and mixed layer depth (Arrigo et al., 2015). In the

89 MGP, Arrigo (2007) found light and nutrient availability to be the most important factors, which will in turn be

90 modulated by changes in mixed layer depth, ice cover and glacial ice melt. Physiological differences in

91 *Phaeocystis antarctica* compared to diatoms mean it can thrive in lower nutrient conditions and lower CO_2

92 levels.

93 The region is affected by various water masses. High Salinity Shelf Water (HSSW) is formed on the shelf in

94 coastal polynyas as a result of sea ice production and the associated brine rejection. HSSW flows out of the shelf

95 through the Adélie sill at 143°E (Fig. 1). Modified Circumpolar Deep Water (mCDW) is a warm, macronutrient-

96 rich and salty water mass which upwells onto the continental shelf through channels in the shelf break. mCDW

97 has been observed to upwell across the shelf break near the Mertz Glacier at 144°E (Williams et al., 2008) (Fig.

98 1). The Antarctic Coastal Current, also known as the East Wind Drift, flows westward often adjacent to ice

99 shelves (Thompson et al., 2018). The Antarctic Surface Water (AASW) is a widespread water mass which

100 extends across the continental shelf and has a surface mixed layer varying from a shallow (ca. 10 m), warmer

101 and fresher layer in summer to a deeper (ca. 100 m), colder layer in winter. This is also transported westward

102 along with the Antarctic Coastal Current (Martin et al., 2017). Surface waters along the Adélie coast have

103 relatively high concentrations of nitrate, silica and phosphorus, with spatially variable levels of Fe which may be

104 due to re-suspension of sediments and calving of ice (Vaillancourt et al., 2003; Sambrotto et al., 2003).

105 **2 Materials and Methods**

106 *Fatty acids*

107 One hundred and thirty-five sediment samples were taken for organic geochemical analyses, sampled at 1 cm

108 intervals in the top 50 cm, 2 cm intervals between 50 and 100 cm, and 5 cm intervals until 458 cm. Lipid

109 extractions were completed at the University of Birmingham using dichloromethane/methanol (3:1 v/v) and

110 ultrasonication. The acid and neutral fractions were separated using an aminopropyl-silica gel column and the

111 FAs eluted using diethyl ether with 4% acetic acid. The acid fraction was derivatized using boron trifluoride (14

112 % in methanol (v/v)) and subsequently cleaned up using a silica gel column and the fatty acid methyl esters

113 (FAMEs) eluted with dichloromethane.

114 FAs were identified using an Agilent 7890B gas chromatograph (GC) coupled to an Agilent 5977A mass

115 selective detector, with a BP5-MS (SGE) column (60m, 320μm internal diameter, 0.25μm film thickness).

116   Helium was used as the carrier gas set at a constant flow rate of 2 ml/min. The MSD was run in scan mode with

117   a scan width of 50 to 800 mass units. Concentrations were quantified using an Agilent 7890B GC-flame

118   ionization detector, using Hydrogen as the carrier gas with a constant flow rate of 2 ml min-1. An Rtx™-200

119   column (105 m, 250μm internal diameter, 0.25μm film thickness) which has a

120   poly(trifluoropropylmethylsiloxane) stationary phase was used for FA analyses to enable the best separation

121   possible. The oven programme was: 70°C, held for 1 min, increased to 150°C at a rate of 30°C/min, increased to

122   320°C at a rate of 3°C/min, then held for 10 minutes. FA concentrations were quantified by addition of a C19

123   alkane as an internal standard, prepared in-house to the concentration of 10 ng/μl. The peak areas of FAs and the

124   internal standard were used to calculate the concentration of each compound.

125   The δ13C composition of fatty acids are described in delta notation:

126               $\delta^{13}C\ (‰) = ((^{12}C/^{13}C)_{sample} / (^{12}C/^{13}C)_{standard} - 1) \times 1000$

127   whereby the standard is Vienna Pee Dee Belemnite. Carbon isotopes were measured using an Agilent 7890A

128   GC coupled to an Isoprime GC5 furnace and an Isoprime 100 isotope ratio mass spectrometer (IRMS). The

129   Isoprime GC5 furnace contained a CuO furnace tube kept at 850°C. Helium was used as the carrier gas set at a

130   constant flow of 1.7 ml/min and CO_2 was used as the reference gas. The GC had a VF-200ms column (60 m,

131   250μm internal diameter, 0.25μm film thickness) which also has a poly(trifluoropropylmethylsiloxane)

132   stationary phase. The oven programme was: 70°C, held for 1 min, increased to 150°C at a rate of 30°C/min,

133   increased to 320°C at a rate of 3°C/min, then held for 5 minutes. Most samples were run using an Agilent 7693

134   autosampler from dilutions of 10 – 100 μl. Where concentrations were very low, samples were dissolved in <10

135   μl and were manually injected. Most samples were run in duplicate except for a few cases where the sample

136   concentration was so low that the entire sample had to be injected in one run.

137   Machine performance was routinely checked using a FA ester mix (F8; Indiana University) containing eight FA

138   compounds. This was run before the start of analysis and after every five duplicate samples.. Errors are based on

139   the difference between duplicate measures and are all within 0.26‰.

140   To correct for the additional carbon added during MeOH derivatization, three FA standards were analysed for

141   their bulk carbon isotope value using an Elementar Pyrocube at the University of Birmingham. Samples were

142   combusted at 920°C before being passed through a reduction column and the isotopic composition of sample

143   gases was determined on an Isoprime continuous flow mass-spectrometer. These samples were then derivatized

144   and then analysed on the GC-IRMS for the $\delta^{13}C$ value of the FAME. The $\delta^{13}C$ of the FA ($\delta^{13}C_{FA}$) and FAME

145   ($\delta^{13}C_{FAME}$) were used to calculate the $\delta^{13}C$ of the MeOH ($\delta^{13}C_{MeOH}$) as follows:

146               $\delta^{13}C_{MeOH} = (nFAME * \delta^{13}C_{FAME}) – (nFA * \delta^{13}C_{FA})$

147   whereby nFAME is the number of carbons in the FAME and nFA is the number of carbons in the FA.

148   δ13CMeOH was calculated to be ca. -40.8‰ and the $\delta^{13}C_{FAME}$ values were corrected using:

149               $\delta^{13}C_{FA} = ((nFAME * \delta^{13}C_{FAME}) + 40.8) / nFA$

150   *HBIs*

151 Two hundred and thirty-four samples were taken every 2 cm over the whole core for highly branched

152 isoprenoids (HBI) alkenes analysis. HBIs were extracted at Laboratoire d'Océanographie et du Climat:

153 Experimentations et Approches Numériques (LOCEAN), separately from the fatty acids, using a mixture of

154 9mL CH_2Cl_2/MeOH (2:1, v:v). 7 hexyl nonadecane (m/z 266) was added as an internal standard during the first

155 extraction steps, following the Belt et al (2007) and Massé et al. (2011) protocols. Several sonication and

156 centrifugation steps were applied in order to fully extract the selected compounds (Etourneau et al., 2013). After

157 drying with N_2 at 35°C, the total lipid extract was fractionated over a silica column into an apolar and a polar

158 fraction using 3 mL hexane and 6 mL CH_2Cl_2/MeOH (1:1, v:v), respectively. HBIs were obtained from the

159 apolar fraction following the procedures reported by Belt et al. (2007) and Massé et al.(2011). After removing

160 the solvent with N_2 at 35°C, elemental sulfur was removed using the TBA (Tetrabutylammonium) sulfite

161 method (Jensen et al., 1977; Riis and Babel, 1999). The obtained hydrocarbon fraction was analyzed within an

162 Agilent 7890A gas chomatograph (GC) fitted with 30 m fused silica Agilent J&C GC column (0.25 mm i.d.,

163 0.25 μm film thickness), coupled to an Agilent 5975C Series mass selective detector (MSD). Spectra were

164 collected using the Agilent MS-Chemstation software. Individual HBIs were identified on the basis of

165 comparison between their GC retention times and mass spectra with those of previously authenticated HBIs

166 (Johns et al., 1999) using the Mass Hunter software. Values are expressed as concentration relative to the

167 internal standard.

168 *Diatoms*

169 One hundred and eighteen samples were taken every 4 cm over the whole core for diatom analyses. Sediment

170 processing and slide preparation followed the method described in Crosta et al. (2020). Diatom counting followed

171 the rules described in Crosta and Koç (2007). Around 350 diatom valves were counted in each sample at a 1000X

172 magnification on a Nikon Eclipse 80i phase contrast microscope. Diatoms were identified to species or species

173 group level. Absolute abundances of diatoms were calculated following the equation detailed in Crosta et al.

174 (2008). The relative abundance of each species was determined as the fraction of diatom species against total

175 diatom abundance in the sample.

176

177 3 Fatty acids within DTGC2011

178 Analysis by GC-MS identified seven dominant saturated FAs within the DTGC2011 samples (Fig. S2). These

179 have carbon chain lengths of C_{16} to C_{26} and only the saturated forms (i.e. no double bonds) were identified.

180 These are predominantly even chain length FAs, with only minor amounts of the C_{17} compound measured

181 (Gilchrist, 2018).

182 3.1 Fatty acid concentrations

183 The C_{19} alkane was used as an internal standard to aid quantification of fatty acid concentrations. However, it

184 should be noted that since this standard was added to samples post-extraction, our concentration estimates are

185 semi-quantitative but can be used to compare concentration changes in different FA compounds.

186 Down core analysis of FA concentrations reveals clear groupings in concentration changes. In the upper part of

187 the core (ca. 3 – 90 cm depth), spanning the last ~78 years, all FA compounds show a similar pattern, with

188   elevated concentrations, broadly decreasing down-core (Fig. 2). Below this, however, two groups clearly

189   diverge. These can be broadly divided into short-chained fatty acids (C_{16} to C_{20}; SCFAs) and long-chained fatty

190   acids (C_{22} to C_{26}; LCFAs). Within these groups, the concentrations of different compounds show similar trends,

191   but the two groups (SCFAs vs LCFAs) show different trends to each other (Gilchrist, 2018). This is confirmed

192   by R^2 values calculated for the linear regression of concentrations of each FA against each other throughout the

193   core (Fig. 3; n = 135, p <0.001). Correlations between the SCFAs have R^2 values between 0.97 and 0.99, while

194   R^2 values of LCFAs range between 0.88 and 0.95. Between the two groups, however, R^2 values are all lower,

195   ranging between 0.50 and 0.77.

196   These distinct groupings suggest that compounds within each group (SCFAs and LCFAs) likely have a common

197   precursor organism or group of organisms, but the two groups themselves have different producers from each

198   other. These producers may in turn thrive during different seasons or within different habitats and thus, the

199   isotopic composition of compounds from these different groups may record different environmental signals.

200   R^2 values were also calculated for samples below 25 cm only (ca. 1587 – 1978 C.E.), to remove correlations

201   associated with preservation changes in the top part of the core (discussed below). Although the R^2 values are

202   not quite as high, they broadly confirm these groupings, with the R^2 values generally being greater within the

203   two groups (n = 73). R^2 values range from 0.93 for the C_{18} with C_{20}, down to 0.07 for the C_{18} and C_{24} (Fig. 4).

204   The C_{18} and C_{24} FAs are the most abundant compounds within the SCFA and LCFA groups, respectively, and

205   also the least correlated with each other both in the whole core ($R^2 = 0.5$) and below 25 cm ($R^2 = 0.07$), which

206   suggests they are the most likely to be produced by different organisms. Furthermore, these two compounds

207   yielded the highest quality isotope measurements, due to their greater concentrations, clean baseline and

208   minimal coeluting peaks (Fig. S2). Thus, these two compounds (C_{18} and C_{24}) will be the focus of analysis and

209   discussion.

210

211   **3.2 Potential sources of the C_{18} fatty acid**

212   Potential sources for the C_{18} FA in core U1357 (recovered from the same site as DTGC2011) are discussed in

213   Ashley et al. (2021) who suggest the prymnesiophyte *Phaeocystis antarctica* to be the most likely main

214   producer. This is based on a) previous studies of FAs produced by microalgae (Dalsgaard et al., 2003), b) the

215   high observed abundance of *P. antarctica* within modern Adélie surface waters (Riaux-Gobin et al., 2011;

216   Sambrotto et al; 2003) and c) comparison between the measured $\delta^{13}C$ values and those reported in the literature

217   for *P. antarctica* (Kopczynska et al., 1995; Wong and Sackett, 1978). Unfortunately, the absence of *P.*

218   *antarctica* in sediments, as it does not biomineralize any test, precludes the direct comparison of down core

219   trends of this species with FAs. *Phaeocystis antarctica* has been found to live within and underneath sea ice

220   before its break up, as well as in open ocean waters (Riaux-Gobin et al., 2013; Poulton et al., 2007), due to its

221   ability to use a wide range of light intensities for energy production (Moisan and Mitchell, 1999).

222   Furthermore, Skerratt et al. (1998) compared the FAs produced by *P. antarctica* and two Antarctic diatoms, in

223   culture samples, and showed that *P. antarctica* produced a much higher percentage of both saturated FAs (C14-

224   C20) and C18 FAs than the diatoms. This supports the hypothesis of *P. antarctica* being a dominant and

225 abundant source of the saturated C_{18} FA in the Adélie basin though minor contributions of C_{18} from other

226 phytoplankton species such as the diatoms and dinoflagellates or even bacteria cannot be excluded (Table S2).

227 **3.3 Potential sources of the C_{24} fatty acid**

228 Long-chain *n*-alkyl compounds, including FAs, are major components of vascular plant waxes and their

229 presence within sediments has commonly been used as a biomarker of terrestrial plants (Pancost and Boot,

230 2004). Although plants such as bryophytes (e.g. mosses) which are present in the Antarctic do also produce

231 LCFAs (Salminen et al., 2018), it is unlikely that FAs from terrestrial plants make a significant contribution to

232 the water column, due to their extremely limited extent on the continent, and the significant distance of the site

233 from other continental sources.

234 However, there is much evidence in the literature for various aquatic sources of LCFAs, a few of which are

235 summarized in Table S2. Although not all of these sources are likely to be present within the coastal waters

236 offshore Adélie Land, it highlights the wide range of organisms which can produce these compounds, and thus

237 suggests that an autochthonous marine source is likely, especially considering the highly productive nature of

238 this region.

239 **3.4 Microbial degradation and diagenetic effects on fatty acid concentration**

240 Both the C_{18} and C_{24} FAs show an overall decrease in concentrations down-core, with significantly higher

241 concentrations in the top 80 cm (representing ~70 years) compared to the rest of the core. Below this point, FAs

242 concentrations variations are attenuated (Fig. 2).

243 Many studies have shown that significant degradation of FAs occurs both within the water column and surface

244 sediments as a result of microbial activity, and that there is preferential break down of both short-chained and

245 unsaturated FA, compared to longer-chained and saturated FA (Haddad et al., 1992; Matsuda, 1978; Colombo et

246 al., 1997). Haddad et al. (1992) studied the fate of FAs within rapidly accumulating (10.3 cm yr^{-1}) coastal

247 marine sediments (off the coast of North Carolina, USA) and showed that the vast majority (ca. 90%) of

248 saturated FAs were lost due to degradation within the top 100 cm (representing ~10 years). Similarly, Matsuda

249 and Koyama (1977) found FA concentrations decrease rapidly within the top 20 cm of sediment (accumulating

250 at 4 mm yr^{-1}) from Lake Suwa, Japan. Assuming similar processes apply to the DTGC2011 sediments, this

251 suggests the declining concentrations within the upper part of the core are largely the result of diagenetic effects

252 such as microbial activity occurring within the surface sediments, and thus do not reflect a real change in

253 production of these compounds in the surface waters.

254 The complete lack of both unsaturated and short chained (fewer than 16 carbon atoms) FA compounds

255 identified within DTGC2011 samples, even within the top layers, suggests that selective breakdown of

256 compounds has already occurred within the water column and on the sea floor (before burial). Wakeham et al.

257 (1984) assessed the loss of FAs with distance during their transport through the water column at a site in the

258 equatorial Atlantic Ocean and estimated that only 0.4 to 2% of total FAs produced in the euphotic zone reached

259 a depth of 389 m, and even less reaching more than 1,000 m depth, the vast majority of material being recycled

260 in the upper water column. Their results also show a significant preference for degradation of both unsaturated

261 and short chained compounds over saturated and longer chain length compounds. Although no studies into the

262 fate of lipids within the water column exist for the Adélie region, the >1,000 m water depth at the core site

263 would provide significant opportunity for these compounds to be broken down during transportation through the
264 water column. It is likely, therefore, that the distribution of compounds preserved within the sediments will not
265 be a direct reflection of production in the surface waters, and explains the preference for saturated FAs with
266 carbon chain lengths of 16 and more. It is also possible that some additional production and contribution of FAs
267 by bacteria occurred during this process (Allen & Bartlett, 2002; Allen et al., 1999; Jónasdóttir, 2019).

268 Although FA concentrations in the top 80 cm of core DTGC2011 are much higher overall than the sediments
269 below and show a broad decline over this section, there is a high level of variability. Concentrations do not
270 decrease uniformly within the top part of the core, as may be expected if concentration change is a first order
271 response to declining microbial activity. The peak in total FAs instead occurs at a depth of 21-22 cm with a
272 concentration more than an order of magnitude higher than in the top layer. This variability creates difficulty in
273 directly determining the effects of diagenesis. However, by 25 cm (ca. 1978 C.E.) the concentrations drop to
274 below 1,000 ng g^{-1} and remain so until 32 cm before increasing again. This may suggest that diagenetic effects
275 of FA concentrations are largely complete by 25 cm (representing ca. 25 years), consistent with results from
276 Haddad et al. (1992) and Matsuda and Koyama (1977), and that subsequent down-core concentration variations
277 predominantly represent real changes in export productivity, resulting from environmental factors. However, the
278 fluctuating nature of concentrations particularly in the youngest sediments means it is difficult to clearly unpick
279 the effects of diagenesis from actual changes in production of these compounds, and a clear cut-off point for
280 diagenetic effects cannot be determined.

281 **3.5 Comparison of fatty acid concentrations with highly branched isoprenoid alkenes**

282 We compare FA concentrations with other organic compounds (whose source is better constrained) in
283 DTGC2011 to better understand FA sources. Direct comparison between different organic compound classes
284 can be made since both are susceptible to similar processes of diagenesis, in contrast to other proxies such as
285 diatoms. In core DTGC2011, concentrations of di- and tri-unsaturated highly branched isoprenoid (HBI) alkenes
286 (referred to as HBI diene and HBI triene, respectively hereafter) were available.

287 In Antarctic marine sediments HBIs have been used as a tool for reconstructing sea ice (Belt et al., 2016, 2017).
288 Smik et al. (2016) compared the concentrations of HBIs in sediment samples offshore East Antarctica from the
289 permanently open-ocean zone (POOZ), the marginal ice zone (MIZ) and the summer sea-ice zone (SIZ). They
290 found the HBI diene reached the highest concentrations in the SIZ and was absent from the POOZ. In contrast,
291 the HBI triene was most abundant in the MIZ, i.e. at the retreating sea ice edge, with much lower concentrations
292 in the SIZ and POOZ. This suggests that the two compounds are produced in contrasting environments but
293 remain sensitive to changes in sea ice.

294 The HBI diene biomarker (or IPSO$_{25}$ for Ice Proxy Southern Ocean with 25 Carbons) is mainly biosynthesised
295 by *Berkeleya adeliensis* (Belt et al., 2016), a diatom which resides and blooms within the sea ice matrix, and
296 thus can be used as a proxy for fast ice attached to the coast. In contrast, the presence of the HBI triene mostly in
297 the MIZ is suggestive of a predominantly pelagic phytoplankton source (e.g. *Rhizosolenia* spp, Massé et al.,
298 2011; Smik et al., 2016; Belt et al., 2017), rather than sea-ice dwelling diatoms (Smik et al., 2016). The fact that
299 HBI triene reached its greatest abundance within the MIZ suggests its precursor organism may thrive in the
300 stratified, nutrient-rich surface waters of the sea-ice edge.

301   One key similarity between both the HBI diene and triene, and the FA concentrations is that the highest

302   concentrations are found in the youngest sediments. These compounds all show broad increases in concentration

303   from 110 cm depth (ca. 1900 C.E) until the top of the core (Fig. 2 and 5). Concentrations of HBIs are also

304   susceptible to degradation through the water column through visible light induced photo-degradation (Belt and

305   Müller, 2013) and diagenetic effects within thesediments including sulphurisation (Sinninghe Damsté et al.,

306   2007), isomerisation and cyclisation (Belt et al., 2000). Thus, it is likely that the elevated concentrations, and

307   thus the similarity between FA and HBI concentrations, is due to the material being fresher and thus less

308   affected by diagenesis, with diagenetic effects having an increasing and progressive impact down to ca. 25cm

309   depth.

310   However, despite an overall increase in HBI and FA concentrations above 110 cm depth, there are clear

311   deviations from this trend. Concentrations of the HBI triene show some broad similarities with FA

312   concentrations. In particular, both the HBI triene and the C_{18} FA have coeval concentration peaks around 1980-

313   88, 1967, 1938, 1961-72, 1848 and 1752 C.E. (Fig. 5). These peaks are offset from the HBI diene

314   concentrations, suggesting that they result from increased production in the surface waters rather than simply

315   changes in preservation. The HBI triene is more susceptible to degradation than the diene (Cabedo Sanz et al.,

316   2016), so while this could explain some of the differences between the diene and triene records, where the triene

317   increases independently of the diene, this is likely to be a genuine reflection of increased production of these

318   compounds at the surface rather than an artefact of preservation processes.

319   This close similarity between the C_{18} FA and HBI triene concentrations (Fig. 5) suggests that the C_{18} may also

320   be produced by an organism associated with the retreating ice edge. *Phaeocystis antarctica* has been proposed

321   as a potential producer of the C_{18} in core U1357B (Ashley et al., 2021). In the Ross Sea, *P. antarctica* has been

322   observed to dominate the phytoplankton bloom during the spring, blooming in deep mixed layers as the sea ice

323   begins to melt, after which diatoms tend to dominate during the summer (Arrigo et al., 1999; Tortell et al., 2011;

324   DiTullio et al., 2000). However, a few studies in the Adélie region suggest this is not the case there. Offshore

325   Adélie Land, *P. antarctica* has been found to only appear late in the spring/early summer, later than many

326   diatom species. During this time, it occurs preferentially within the platelet ice and under-ice water (Riaux-

327   Gobin et al., 2013). Furthermore, Sambrotto et al. (2003) observed a surface bloom of *P. antarctica* near the

328   Mertz Glacier (Fig. 1) during the summer months, in very stable waters along the margin of fast ice and Riaux-

329   Gobin et al. (2011) found *P. antarctica* to be abundant in the coastal surface waters eight days after ice break up.

330   This indicates an ecological niche relationship with cold waters and ice melting conditions. This might explain

331   the close similarity between the C_{18} and HBI triene concentrations, both produced by organisms occupying a

332   similar habitat at the ice edge.

333   The C_{24} FA record also shows some similarity with the HBI triene record. This appears to be mostly in the top

334   part of the core where the highest concentrations are found. The reason for this resemblance is unclear,

335   especially considering the lack of correlation between the C_{24} and C_{18} FA concentrations. However, it may relate

336   to the progressive effect of diagenesis through the core. There is less similarity between the C24 and both the

337   HBI triene also HBI diene, (compared to the coherence between C18 FA and HBI triene), which suggests that

338   the C24 FA is predominantly produced by an organism which is not associated with sea ice, and thus instead

339   with more open waters. Seventy-three diatom species were encountered in core DTGC2011 (Campagne, 2015),

with *Fragilariopsis curta* and *Chaetoceros* resting spores being the most abundant. However, trends in diatom abundances do not show any clear correlations with the C_{18} or C_{24} FA concentrations. While this would lend support to the hypothesis that diatoms are not the main producers of these compounds, the differing effects of diagenesis on the preservation of diatoms and lipids could also explain some of the differences in observed concentrations, particularly in the upper part of the core. The known producer of the HBI diene, *Berkeleya adeliensis*, for example, was not recorded within the core, likely due to their lightly silicified frustules which are more susceptible to dissolution (Belt et al., 2016). Therefore, despite the lack of a correlation between diatom abundances and FA concentrations, we cannot entirely rule out the possibility of a minor contribution of FAs by diatoms.

4 Carbon isotopes of fatty acids

Down-core changes in $\delta^{13}C$ for the C_{18} and C_{24} FAs ($\delta^{13}C_{18FA}$ and $\delta^{13}C_{24FA}$, respectively) (Fig. 7) clearly show different trends, with very little similarity between them ($R^2 = 0.016$). This further supports the idea that these compounds are being produced by different organisms, and thus are recording different information.

The mean carbon isotope value of $\delta^{13}C_{18FA}$ of -29.8 ‰ in core U1357 from the same site (Ashley et al., 2021) is suggestive of a pelagic phytoplankton source (Budge et al., 2008). In core DTGC2011 the mean values of $\delta^{13}C_{18FA}$ and $\delta^{13}C_{24FA}$ are -26.2 ‰ and -27.6 ‰, respectively. Though more positive, these values are still within the range of a phytoplankton source. Additionally, we tentatively suggest that the 0.5‰ more positive $\delta^{13}C_{18FA}$ mean value over the $\delta^{13}C_{24FA}$ may indicate the contribution of sea-ice dwelling algae producers, since carbon fixation occurring within the semi-closed system of the sea ice will lead to a higher degree of CO_2 utilisation than in surrounded open waters (Henley et al., 2012). Although no studies on FA $\delta^{13}C$ of different organisms are available for the Southern Ocean, Budge et al. (2008) measured the mean $\delta^{13}C$ value of C_{16} FA from Arctic sea-ice algae (-24.0 ‰) to be 6.7 ‰ higher than pelagic phytoplankton (-30.7 ‰) from the same region.

The higher $\delta^{13}C$ of the C_{18} FA could therefore be indicative of *P. antarctica* living partly within the sea ice, e.g. during early spring before ice break up. The more negative $\delta^{13}C_{24FA}$ suggests it is more likely to be produced by phytoplankton predominantly within open water.

4.1 Controls on $\delta^{13}C_{FA}$

The $\delta^{13}C_{18FA}$ record shows a broadly increasing trend towards more positive values from ca. 1587 until ca. 1920 C.E., with short term fluctuations of up to ~4 ‰ superimposed on this long-term trend (Fig. 7). This is followed by a period of higher variability with a full range of 5.6 ‰ until the most recent material (ca. 1999 C.E.), with more negative $\delta^{13}C$ values between 1921 and 1977 C.E. and a rapid shift toward more positive values thereafter. In contrast, the $\delta^{13}C_{24FA}$ record overall shows a weak, negative trend, with large decadal fluctuations of up to 4.6 ‰, with a more pronounced negative trend after ca. 1880 C.E. (Fig. 7).

Below we consider the various factors which may control the carbon isotope value of algal biomarkers produced in the surface waters. Down-core changes in FA $\delta^{13}C$ are likely to be a function of either the $\delta^{13}C$ of the dissolved inorganic carbon (DIC) source, changes in the species producing the biomarkers, diagenesis or changing photosynthetic fractionation (ε_p). The next section outlines the potential influence of these factors may have in order to assess the mostly likely dominant driver of FA $\delta^{13}C$.

 4.1.1 Isotopic composition of DIC

378 The $\delta^{13}C$ of the DIC source can be affected by upwelling or advection of different water masses, or the $\delta^{13}C$ of

379 atmospheric CO_2. Around the Antarctic, distinct water masses have unique carbon, hydrogen and oxygen

380 isotope signatures and thus isotopes can be used as water mass tracers (e.g. Mackensen, 2001, Archambeau et

381 al., 1998). In the Weddell Sea for example, Mackensen (2001) determined the $\delta^{13}C$ value of eight water masses,

382 which ranged from 0.41 ‰ for Weddell Deep Water, sourced from CDW, to 1.63 ‰ for AASW. A similar

383 range of ~1.5 ‰ was identified in water masses between the surface and ~5,500 m depth along a transect from

384 South Africa to the Antarctic coast (Archambeau et al., 1998). Assuming similar values apply to these water

385 masses offshore Adélie Land, this range in values would be insufficient to explain the ~5 ‰ variation of $\delta^{13}C$

386 recorded by both C_{18} and C_{24} FA, even in the situation of a complete change in water mass over the core site.

387 Furthermore, site DTGC2011, located within a 1,000 m deep depression and bounded by the Adélie Bank to the

388 north, is relatively sheltered from direct upwelling of deep water (Fig. 1). Though inflow of mCDW has been

389 shown to occur within the Adélie Depression to the east of the bank (Williams and Bindoff, 2003) and possibly

390 within the Dumont d'Urville Trough, only very small amplitude changes in $\delta^{13}C$ of benthic foraminifera,

391 tracking upper CDW, have been observed over the Holocene in Palmer Deep, West Antarctica (Shevenell and

392 Kennett, 2002). Although from a different location, this argues against large changes in the isotopic composition

393 of the source of mCDW.

394 Changes in the $\delta^{13}C$ of atmospheric CO_2, which is in exchange with the surface waters could also have the

395 potential to drive changes in the $\delta^{13}C$ of algal biomarkers. Over the last ca. 200 years, the anthropogenic burning

396 of fossil fuels has released of a large amount of CO_2 depleted in ^{13}C, meaning that the $\delta^{13}C$ of CO_2 has

397 decreased by ca. 1.5 ‰, as recorded in the Law Dome ice core. Prior to this, however, the $\delta^{13}C$ of CO_2 in the

398 atmosphere remained relatively stable, at least for the last thousand years (Francey et al., 1999). Therefore, this

399 could potentially drive the $\delta^{13}C$ of algal biomarkers towards more negative values within the last 200 years, but

400 this could not explain the full variation of ~5-6 ‰ in FA $\delta^{13}C$ measured throughout the core. Although the C_{24}

401 $\delta^{13}C$ shows a slight decrease over the last ca. 100 years, this is preceded by increasing $\delta^{13}C$, while the C_{18} $\delta^{13}C$

402 displays no clear trend over the last 200 years. If atmospheric CO_2 was a key driver of fatty acid $\delta^{13}C$, we would

403 expect both compounds to respond together, showing a trend towards more negative values over the last 200

404 years which neither of them do. This suggests that the effect of changing $\delta^{13}C$ of atmospheric CO_2 is

405 insignificant compared to local and regional inter-annual variations as a result of other environmental drivers

406 (discussed below).

407 *4.1.2 Changing species*

408 A shift in the organisms producing the FA could also affect $\delta^{13}C$ where species have different fractionation

409 factors. For example, changing diatom species have been shown to have an effect on bulk organic matter $\delta^{13}C$ in

410 core MD03-2601, offshore Adélie Land, over the last 5 ka (Crosta et al., 2005). However, the bulk organic

411 matter might have contained other phytoplankton groups than diatoms with drastically different $\delta^{13}C$ values and

412 fractionation factors. Here we measured $\delta^{13}C$ of individual biomarkers, produced by a more restricted group of

413 phytoplankton groups (possibly restricted to a few dominant species) compared to bulk $\delta^{13}C$. As discussed

414 above, the C_{18} appears to be produced predominantly by *P. antarctica,* whereas diatoms do not tend to produce

415 high proportions of this compound (Dalsgaard et al., 2003).

4.1.3 Effect of diagenesis on lipid $\delta^{13}C$

Sun et al. (2004) studied the carbon isotope composition of FAs during 100 days of incubation in both oxic and anoxic seawater. They observed a shift towards more positive values in FA $\delta^{13}C$, ranging between 2.6 ‰ for the $C_{14:0}$ and as much as 6.9‰ in the $C_{18:1}$, under anoxic conditions. This suggests that diagenesis could affect FA $\delta^{13}C$ in core DTGC2011. However, these observed changes are rapid (days to months), occurring on timescales which are unresolvable in the FA $\delta^{13}C$ record (annual to decadal), and thus may have no effect on the trends observed in our record. Based on concentration data discussed above, it seems that diagenetic overprint is largely complete by ~25 cm (Fig. 2). In the top 25 cm of the core (ca. 1978 – 1998 C.E.), the $\delta^{13}C_{24FA}$ values increase by ~2.5 ‰, downward (R^2 = 0.63, n = 11) while the $\delta^{13}C_{18FA}$ values display a large variation with no overall trend (R^2 = 0.12, n = 20). If diagenesis was driving the changes in $\delta^{13}C$, it is likely that this trend would be observed in all FA compounds.

Taken together, it appears that neither changes in the $\delta^{13}C$ of the DIC, changing phytoplankton groups nor diagenesis can fully explain the variation of FA $\delta^{13}C$ recorded within DTGC2011. Therefore, we hypothesise that changes in ε_p are the main driver of FA $\delta^{13}C$.

4.2 Controls on photosynthetic fractionation (ε_p)

There is a positive relationship between ε_p in marine algae and dissolved surface water $CO_{2(aq)}$ concentration (Rau et al., 1989). As a result, higher $\delta^{13}C$ values are hypothesised to reflect lower surface water $CO_{2(aq)}$ and vice versa. Popp et al. (1999) showed a strong negative correlation between CO_2(aq) and $\delta^{13}C$ of suspended particulate organic matter across a latitudinal transect in the Southern Ocean, suggesting that changes in surface water CO_2(aq) can explain a large amount of the variation in $\delta^{13}C$. Changes in surface water $CO_{2(aq)}$ concentration in turn may be driven by various factors, including changing atmospheric CO_2 (Fischer et al., 1997), wind-driven upwelling of deep, carbon-rich water masses (Sigman and Boyle, 2000; Takahashi et al., 2009), sea-ice cover (Henley et al., 2012) and/or primary productivity (Villinski et al., 2008). Thus, determining the main driver(s) of surface water CO_2 changes offshore Adélie Land should enable interpretation of the DTGC2011 FA $\delta^{13}C$ records.

4.2.1 Sea ice

Brine channels within sea ice have very low CO_2 concentrations and a limited inflow of seawater. Carbon isotopic fractionation of algae living within these channels has been shown to be greatly reduced compared to organisms living in the surrounding open waters (Gibson et al., 1999), leading to elevated $\delta^{13}C$ values. It is thus possible that, under conditions of high sea-ice cover, enhanced FA contribution from sea-ice algae leads to elevated sedimentary $\delta^{13}C$ values. HBI diene concentrations within DTGC2011 show a much greater presence of fast ice at the core site ca. 1960 C.E (Fig. 5). However, during this time there is no clear elevation in $\delta^{13}C$ concentrations in either $\delta^{13}C_{18FA}$ or $\delta^{13}C_{24FA}$, both instead showing generally lower $\delta^{13}C$ values. In fact, $\delta^{13}C_{18FA}$ shows the lowest values of the whole record between 1925 and 1974 C.E., during which sea ice, as recorded by the HBI diene, is at its highest level. This suggests that inputs in sea-ice algae at this time are not driving changes in FA $\delta^{13}C$.

The DTGC2011 core site sits proximal to the Dumont D'Urville polynya, which has a summer area of 13.02 x 10^3 km^2 and a winter area of 0.96 x 10^3 km^2 (Arrigo and van Dijken, 2003). Changes in the size of the polynya

454 both on seasonal and inter-annual time scales will affect air-sea CO_2 exchange and thus also surface water CO_2

455 concentration. A reduced polynya may lead to greater supersaturation of CO_2 in the surface waters due to

456 reduced outgassing, allowing CO_2 to build up below the ice, leading to lower $\delta^{13}C$ values of algal biomarkers

457 produced in that habitat (Massé et al., 2011). Thus changes in the extent of sea ice may also effect FA $\delta^{13}C$.

458 *4.2.2 Observed trends in surface water $CO_{2(aq)}$*

459 If the trend in surface water $CO_{2(aq)}$ paralleled atmospheric CO_2, with an increase of over 100 ppm over the last

460 200 years (MacFarling Meure et al., 2006), we might expect phytoplankton to exert a greater fractionation

461 during photosynthesis in response to elevated surface water $CO_{2(aq)}$ concentration, resulting in more negative

462 $\delta^{13}C$ values. Taking into account the decline in atmospheric $\delta^{13}CO_2$ over the same period would further enhance

463 the reduction in phytoplankton $\delta^{13}C$. Fischer et al. (1997) looked at the $\delta^{13}C$ of both sinking matter and surface

464 sediments in the South Atlantic and suggested that, since the preindustrial, surface water $CO_{2(aq)}$ has increased

465 much more in the Southern Ocean than in the tropics. They estimated that a 70 ppm increase in $CO_{2(aq)}$ in

466 surface waters of 1°C would decrease phytoplankton $\delta^{13}C_{org}$ by ca. 2.7‰, and up to 3.3‰ $\delta^{13}CO_2$ change are

467 included, between preindustrial and 1977-1990. However, sea ice cover and summer primary productivity are

468 likely to be much higher off Adélie Land than in the South Atlantic, both of which will affect air-sea gas

469 exchange.

470 Shadwick et al. (2014) suggest that surface water CO_2 should track the atmosphere in the Mertz Polynya region,

471 despite the seasonal ice cover limiting the time for establishing equilibrium with the atmosphere. They

472 calculated wintertime CO_2 in the shelf waters of the Mertz Polynya region, offshore Adélie Land (Fig. 1),

473 measuring ca. 360 ppm in 1996, ca. 396 ppm in 1999, and ca. 385 ppm in 2007, while atmospheric CO_2 at the

474 South Pole was 360, 366 and 380 ppm, respectively (Keeling et al., 2005). Based on the 1996 and 2007 data

475 only, an increase in CO_2 of ca. 25 ppm is observed over these 11 years, coincident with the 20 ppm atmospheric

476 CO_2 increase over this time period. However, high interannual variability (± ca. 30 ppm) is evident (e.g. 396

477 ppm in 1999) suggesting that other factors, particularly upwelling, may override this trend. The latter was also

478 suggested by Roden et al. (2013) based on winter surface water measurements in Prydz Bay, indicating that

479 decadal-scale carbon cycle variability is nearly twice as large as the anthropogenic CO_2 trend alone.

480 During the austral winter, upwelling of deep water masses causes CO_2 to build up in the surface waters, and sea

481 ice cover limits gas exchange with the atmosphere (Arrigo et al., 2008; Shadwick et al., 2014). Although only

482 limited data, the measurements by Shadwick et al. (2014) suggest slight supersaturation, of up to 30 ppm, occurs

483 in the winter due to mixing with carbon-rich subsurface water, but with high interannual variability. This is

484 compared to undersaturation of 15 to 40 ppm during the summer as a result of biological drawdown of CO_2.

485 Roden et al. (2013) also observed varying levels of winter supersaturation in Prydz Bay, East Antarctica, with

486 late winter CO_2 values of 433 ppm in 2011 (45 μatm higher than atmospheric CO_2), and suggested that

487 intrusions of C-rich mCDW onto the shelf may play a part in this. Similarly, winter surface water CO_2 of 425

488 ppm has been measured by Sweeney (2003) in the Ross Sea, before being drawn down to below 150 ppm in the

489 summer as phytoplankton blooms develop.

490 Enhanced upwelling of deep carbon-rich waters in the Southern Ocean are thought to have played a key role in

491 the deglacial rise of atmospheric CO_2, increasing CO_2 concentrations by ~80 ppm (Anderson et al., 2009; Burke

and Robinson, 2012). Changes in upwelling offshore Adélie Land could therefore drive some interannual variability in surface water CO_2 and hence FA $\delta^{13}C$ in DTGC2011. However, upwelling tends to be stronger during the winter months, when sea-ice formation and subsequent brine rejection drive mixing with deeper C-rich waters. At this time, heavy sea-ice cover limits air-sea gas exchange and enhances CO_2 supersaturation in regional surface waters (Shadwick et al., 2014). In contrast, the phytoplankton producing FA thrive during the spring and summer months during which CO_2 is rapidly drawn down and the surface waters become undersaturated. However, upwelling cannot be discarded as a possible contributor to surface water CO_2 change. However, the core site is in a relatively sheltered area and is probably not affected by significant upwelling.

Based on these studies, changes in atmospheric CO_2 concentration and $\delta^{13}C$ of the source appear to be unlikely to be a dominant driver of the FA $\delta^{13}C$ record, with interannual variations driven by other factors overriding any longer-term trend. There is also no clear anthropogenic decline in the FA $\delta^{13}C$ record over the last 200 years, which supports this hypothesis.

4.2.3 Productivity

Given that changes in atmospheric CO_2, source signal, sea ice algae or diagenesis seem unable to explain the full range of variability seen in the FA $\delta^{13}C$ record, the most plausible driver appears to be changes in surface water primary productivity. Coastal polynya environments in the Antarctic are areas of very high primary productivity (Arrigo and van Dijken, 2003). The DTGC2011 core site sits near to the Dumont D'Urville polynya, and is just downstream of the larger and more productive MGP (Arrigo and van Dijken, 2003). In large polynyas such as the Ross Sea, primary productivity leads to intense drawdown of CO_2 in the surface waters, resulting in reduced fractionation by the phytoplankton during photosynthesis (Villinski et al., 2008). In the Ross Sea, surface water CO_2 has been observed to drop to below 100 ppm during times of large phytoplankton blooms (Tortell et al., 2011) demonstrating that primary productivity can play a key role in controlling surface water CO_2 concentrations in a productive polynya environment. Arrigo et al. (2015) found the MGP to be the 8th most productive polynya in the Antarctic (out of 46) based on total net primary productivity during their sampling period, and Shadwick et al. (2014) observed CO_2 drawdown in the MGP during the summer months.

Therefore, we suggest that FA $\delta^{13}C$ signals recorded in DTGC2011 is predominantly a signal of surface water CO_2 driven by primary productivity. Indeed, the potential for the $\delta^{13}C$ of sedimentary lipids to track surface water primary productivity has been recognised in the highly productive Ross Sea polynya. High variability in surface water CO_2 values have been measured across the polynya during the summer months (December – January), ranging from less than 150 ppm in the western Ross Sea near the coast, to >400 ppm on the northern edge of the polynya. This pattern was closely correlated with diatom abundances, indicating intense drawdown of CO_2 in the western region where diatom abundances were highest (Tortell et al., 2011). This spatial variation in productivity is recorded in particulate organic carbon (POC) $\delta^{13}C$, and is also tracked in the surface sediments by total organic carbon (TOC) $\delta^{13}C$ and algal sterol $\delta^{13}C$, all of which show significantly higher values in the western Ross Sea. This spatial pattern in sterol $\delta^{13}C$ was concluded to be directly related to CO_2 drawdown at the surface, resulting in average sterol $\delta^{13}C$ values varying from -27.9‰ in the west, where productivity is greatest, down to -33.5‰ further offshore (Villinski et al., 2008).

529 A similar relationship is evident in Prydz Bay, where POC $\delta^{13}C$ was found to be positively correlated with POC

530 concentration and negatively correlated with nutrient concentration, indicating greater drawdown of CO_2 and

531 nutrients under high productivity levels (Zhang et al., 2014).

532 This suggests it is possible to apply FA $\delta^{13}C$ as a palaeoproductivity indicator in the highly productive Adélie

533 polynya environment. However, it is important to constrain the most likely season and habitat being represented,

534 since phytoplankton assemblages vary both spatially (e.g. ice edge or open water) and temporally (e.g. spring or

535 summer). The incredibly high sedimentation rate (1-2 cm yr^{-1}) within the Adélie Basin is thought to result, on

536 top of regional high productivity, from syndepositional focusing processes bringing biogenic debris from the

537 shallower Adélie and Mertz banks to the ca. 1,000 m deep basin (Escutia et al., 2011). Thus, it is likely that core

538 DTGC2011 contains material from a wide area, including both the Mertz and Dumont d'Urville polynyas, and

539 areas both near the coast and further offshore, meaning it is quite possible that the C_{18} and C_{24} FAs are

540 integrating palaeoproductivity changes weighted towards different regional environments, which would explain

541 their different trends. Furthermore, surface water CO_2 can vary spatially, such as in the Ross Sea polynya where

542 Tortell et al. (2011) measured surface water CO_2 values ranging between 100 and 400 ppm. Thus, it is likely

543 that these two areas offshore Adélie Land where the C_{18} and C_{24} FAs are being produced will also have differing

544 surface water CO_2 concentrations and trends.

4.3 Comparison of fatty acid $\delta^{13}C$ with other proxy data

546 Comparison of down-core variations in FA $\delta^{13}C$ with other proxy data can also be used to decipher the main

547 signal recorded. Comparison between $\delta^{13}C_{24FA}$ and the major diatom species abundances within the core

548 (*Fragilariopsis kerguelensis*, *Fragilariopsis curta*, *Fragilariopsis rhombica*, *Fragilariopsis cylindrus*,

549 *Chaetoceros* resting spores) shows a reasonably close coherence with *Fragilariopsis kerguelensis,* particularly

550 since ~1800 C.E. (Fig. 6). *Fragilariopsis kerguelensis* is an open water diatom species and one of the most

551 dominant phytoplankton species offshore Adélie Land (Chiba et al., 2000), reaching its peak abundance in the

552 summer (Crosta et al., 2007). This suggests that the C_{24} FA is being produced during the summer months and, as

553 such, is reflecting productivity in more open waters. The $\delta^{13}C_{24FA}$ record does not show any similarity to the sea-

554 ice records, as inferred by HBI diene concentrations and abundances of *Fragilariopsis curta* (Fig. 6 and 7), here

555 again suggesting that these compounds are being produced in open water during the summer months after sea

556 ice has retreated.

557 As discussed above, *P. antarctica* is a likely producer for the C_{18} FA, a prymnesiophyte algae which has been

558 observed in the Adélie region in summer months residing predominantly along the margin of fast ice, but also

559 further offshore (Riaux-Gobin et al., 2013, 2011; Vaillancourt et al., 2003). The aversion of *F. kerguelensis* to

560 sea ice (and thus also the C_{24} FA producer) in contrast to *P. antarctica*, may explain the clear lack of coherence

561 in the down-core trends in $\delta^{13}C_{18FA}$ and $\delta^{13}C_{24FA}$ (Fig. 7). Thus, we hypothesise that $\delta^{13}C_{18FA}$ is recording surface

562 water CO_2 driven by productivity in the MIZ, whilst $\delta^{13}C_{24FA}$ is recording surface water CO_2 in more open

563 water, further from the sea-ice edge.

564 HBI diene concentrations indicate elevated fast ice cover between ~1919 and 1970 C.E., with a particular peak

565 between 1942 and 1970 C.E., after which concentrations rapidly decline and remain low until the top of the core

566 (Fig. 7). Abundances of *F. curta*, used as a sea-ice proxy, similarly show peaks at this time indicate increased

567   sea-ice concentration (Campagne, 2015) (Fig. 7). $\delta^{13}C_{18FA}$ indicates a period of low productivity between ~1922

568   and 1977 C.E., broadly overlapping with this period of elevated fast ice concentration (Fig. 7), with a mean

569   value of -27.12‰. This is compared to the mean value of -26.23‰ in the subsequent period (~1978 to 1998

570   C.E.) during which HBI diene concentration remain low (Fig. 7). This suggests that productivity in the coastal

571   region was reduced, while sea-ice concentrations were high. This might be expected during a period of

572   enhanced ice cover – perhaps representing a reduction in the amount of open water, or a shorter open water

573   season – since the majority of productivity generally takes place within open water (Wilson et al., 1986).

574   Furthermore, $\delta^{13}C_{18FA}$ shows a broad similarity with *Chaetoceros* resting spores (CRS) on a centennial scale,

575   with lower productivity at the start of the record, ca. 1587 to 1662 C.E., followed by an increase in both proxies

576   in the middle part of the record, where $\delta^{13}C_{18FA}$ becomes relatively stable and CRS reaches its highest

577   abundances of the record. This is then followed in the latter part of the record, after ca. 1900 C.E., by both

578   proxies displaying lower values overall. CRS are associated with high nutrient levels and surface water

579   stratification along the edge of receding sea ice, often following high productivity events (Crosta et al., 2008).

580   The broad similarity to CRS, with lower values recorded during periods of high sea-ice concentrations, suggests

581   that $\delta^{13}C_{18FA}$ is similarly responding to productivity in stratified water at the ice edge. This supports the

582   hypothesis that $\delta^{13}C_{18FA}$ is recording primary productivity in the MIZ. Little similarity is evident between the

583   fatty acid isotope records and *F. cylindrus* and *F. rhombica*.

584   **5 Conclusions**

585   FAs identified within core DTGC2011, recovered from offshore Adélie Land, were analysed for their

586   concentrations and carbon isotope compositions to assess their utility as a palaeoproductivity proxy in an

587   Antarctic polynya environment. The C_{18} and C_{24} compounds yielded the best isotope measurements and show

588   very different $\delta^{13}C$ trends, suggesting they are being produced by different species in different habitats and/or

589   seasons. Although we have made parsimonious interpretations, there are clearly uncertainties in interpreting the

590   FA $\delta^{13}C$, and, as such various assumptions have been made. The primary producers of the C_{18} and especially the

591   C_{24} FAs are a key source of uncertainty. Because these are general biomarkers, produced by many organisms, it

592   is impossible to constrain entirely to one producer class. But with further work in the region, it could be possible

593   further elucidate the most likely contributors. The possibility of inputs of FAs from multiple sources, in

594   particular from organisms further up the food chain, has consequences for their interpretation since this could

595   mean the $\delta^{13}C$ FA is not fully reflecting just surface water conditions. Other key uncertainties are the magnitude

596   of upwelling of CO_2 at the site in comparison to drawdown by phytoplankton, and the potential role of changes

597   in air-sea CO_2 exchange.

598

599   Despite this, we argue that FA $\delta^{13}C$ has the potential to be used as a productivity proxy, but would be best used

600   in parallel with other environmental proxies such as diatoms abundances or HBIs. Comparison with other proxy

601   data and information from previous studies suggests that the C_{18} compound may be predominantly produced by

602   *P. antarctica*, with $\delta^{13}C_{18FA}$ reflecting productivity changes in the marginal ice zone, where it is sensitive to

603   changes in ice cover. In contrast, $\delta^{13}C_{24FA}$, which compares well with abundances of the open water diatom *F*

604 *kerguelensis,* may be reflecting summer productivity further offshore, in open waters where it is less sensitive to

605 fast ice changes. The use of $\delta^{13}C$ analysis of multiple FA compounds, as opposed to individual compounds or

606 bulk isotope analysis, allows a more detailed insight into the palaeoproductivity dynamics of the region, with the

607 potential to separate productivity trends within different habitats.

608

609 **References**

610 Allen, E. E. & Bartlett, D. H. (2002) Structure and regulation of the omega-3 polyunsaturated fatty acid synthase

611 genes from the deep-sea bacterium Photobacterium profundum strain SS9The GenBank accession numbers for

612 the sequences reported in this paper are AF409100 and AF467805. Microbiology 148, pp. 1903-1913.

613 Allen, E. E., Facciotti, D. & Bartlett, D. H. (1999), Monounsaturated but Not Polyunsaturated Fatty Acids Are

614 Required for Growth of the Deep-Sea Bacterium Photobacterium profundum SS9 at High Pressure and Low

615 Temperature. Applied and Environmental Microbiology 65, 1710-1720, doi:10.1128/aem.65.4.1710-1720.1999.

616 Anderson, R.F., Ali, S., Bradtmiller, L.I., et al. (2009) Wind-driven upwelling in the Southern Ocean and the

617 deglacial rise in atmospheric CO2. *Science (New York, N.Y.)*, 323 (5920): 1443–1448.

618 doi:10.1126/science.1167441.

619 Archambeau, A.S., Pierre, C., Poisson, A., et al. (1998) Distributions of oxygen and carbon stable isotopes and

620 CFC-12 in the water masses of the Southern Ocean at 30°E from South Africa to Antarctica: Results of the

621 CIVA1 cruise. *Journal of Marine Systems*, 17 (1–4): 25–38. doi:10.1016/S0924-7963(98)00027-X.

622 Arrigo, K. R. (2007) 'Chapter 7 Physical Control of Primary Productivity in Arctic and Antarctic Polynyas',

623 Elsevier Oceanography Series, 74(06), pp. 223–238. doi: 10.1016/S0422-9894(06)74007-7.Arrigo, K.R., van

624 Dijken, G. and Long, M. (2008) Coastal Southern Ocean: A strong anthropogenic CO2 sink. *Geophysical*

625 *Research Letters*, 35 (21): 1–6. doi:10.1029/2008GL035624.

626 Arrigo, K.R. and van Dijken, G.L. (2003) Phytoplankton dynamics within 37 Antarctic coastal polynya systems.

627 *Journal of Geophysical Research*, 108 (C8): 3271. doi:10.1029/2002JC001739.

628 Arrigo, K.R., van Dijken, G.L. and Strong, A.L. (2015) Environmental controls of marine productivity hot spots

629 around Antarctica. *Journal of Geophysical Research: Oceans*, pp. 2121–2128. doi:10.1002/jgrc.20224.

630 Arrigo, K.R., Robinson, D.H., Worthen, D.L., et al. (1999) Community Phytoplankton Structure and the

631 Drawdown of and CO2 in the Nutrients Southern Ocean. *Science*, 283 (5400): 365–367.

632 Ashley, K., McKay, R., Etourneau, J., Jimenez-Espejo, F.J., Condron, A., Albot, A., Crosta, X., Riesselman, C.,

633 Seki, O., Masse, G., Golledge, N.R., Gasson, E., Lowry, D.P., Barrand, N.E., Bertler, N., Escutia, C., Dunbar,

634 R., Bendle, J. (2021), Mid-Holocene Antarctic sea-ice increase driven by marine ice sheet retreat, Climate of the

635 Past, 17, 1–19.

636 Belt, S.T., Allard, W.G., Rintatalo, J., et al. (2000) Clay and acid catalysed isomerisation and cyclisation

637 reactions of highly branched isoprenoid (HBI) alkenes: Implications for sedimentary reactions and distributions.

638 *Geochimica et Cosmochimica Acta*, 64 (19): 3337–3345. doi:10.1016/S0016-7037(00)00444-0.

639   Belt, S.T., Brown, T.A., Smik, L., et al. (2017) Identification of C25 highly branched isoprenoid (HBI) alkenes
640   in diatoms of the genus Rhizosolenia in polar and sub-polar marine phytoplankton. *Organic Geochemistry*, 110:
641   65–72. doi:10.1016/j.orggeochem.2017.05.007.

642   Belt, S.T. and Müller, J. (2013) The Arctic sea ice biomarker IP 25 : a review of current understanding ,
643   recommendations for future research and applications in palaeo sea ice reconstructions. *Quaternary Science*
644   *Reviews*, 79: 9–25. doi:10.1016/j.quascirev.2012.12.001.

645   Belt, S.T., Smik, L., Brown, T.A., et al. (2016) Source identification and distribution reveals the potential of the
646   geochemical Antarctic sea ice proxy IPSO25. *Nature Communications*, 7: 1–10. doi:10.1038/ncomms12655.

647   Beucher, C., Tre, P., Hapette, A., et al. (2004) Intense summer Si-recycling in the surface Southern Ocean., 31:
648   0–3. doi:10.1029/2003GL018998.

649   Budge, S.M., Wooller, M.J., Springer, A.M., et al. (2008) Tracing carbon flow in an arctic marine food web
650   using fatty acid-stable isotope analysis. *Oecologia*, 157 (1): 117–129. doi:10.1007/s00442-008-1053-7.

651   Burke, A. and Robinson, L.F. (2012) The Southern Ocean's Role in Carbon Exchange During the Last
652   Deglaciation. *Science*, 335: 557–561.

653   Cabedo Sanz, P., Smik, L. and Belt, S.T. (2016) On the stability of various highly branched isoprenoid (HBI)
654   lipids in stored sediments and sediment extracts. *Organic Geochemistry*, 97: 74–77.
655   doi:10.1016/j.orggeochem.2016.04.010.

656   Campagne, P. (2015) *Étude de la variabilité des conditions océanographiques et climatiques en Antarctique de*
657   *l'Est (Terre Adélie-Georges V) au cours de l'Holocène tardif et de la période instrumentale*. L'Université de
658   Bordeaux.

659   Ceccaroni, L., Frank, M., Frignani, M., Langone, L., Ravaioli, M. & Mangini, A. 1998. Late Quaternary
660   fluctuations of biogenic component fluxes on the continental slope of the Ross Sea, Antarctica. *Journal of*
661   *Marine Systems*, **17**, 515–525.

662   Chiba, S., Hirawake, T., Ushio, S., et al. (2000) An overview of the biological/oceanographic survey by the
663   RTV Umitaka-Maru III off Adelie Land, Antarctica in January-February 1996. *Deep-Sea Research Part II:*
664   *Topical Studies in Oceanography*, 47 (12–13): 2589–2613. doi:10.1016/S0967-0645(00)00037-0.

665   Colombo, J.C., Silverberg, N. and Gearing, J.N. (1997) Lipid biogeochemistry in the Laurentian Trough--ll.
666   Changes in composition of fatty acids, sterols and aliphatic hydrocarbons during early diagenesis. *Org.*
667   *Geochem.*, 26 (3): 257–274.

668   Crosta, X., Crespin, J., Billy, I., et al. (2005) Major factors controlling Holocene d13Corg changes in a seasonal
669   sea-ice environment, Adelie Land, East Antarctica. *Global Biogeochemical Cycles*, 19 (4).
670   doi:10.1029/2004GB002426.

671   Crosta, X., Debret, M., Denis, D., et al. (2007) Holocene long- and short-term climate changes off Adelie Land,
672   East Antarctica. *Geochemistry Geophysics Geosystems*, 8 (11): n/a-n/a. doi:10.1029/2007GC001718.

673 Crosta X, Shukla S.K., Ther O., Ikehara M., Yamane M., Yokoyama Y. (2020) Last Abundant Appearance

674 Datum of Hemidiscus karstenii driven by climate change. *Marine Micropaleontology*,

675 doi:10.1016/j.marmicro.2020.101861.

676 Dalsgaard, J., St. John, M., Kattner, G., et al. (2003) Fatty acid trophic markers in the pelagic marine

677 environment. *Advances in Marine Biology*. 46 pp. 225–340. doi:10.1016/S0065-2881(03)46005-7.

678 DiTullio, G.R., Grebmeier, J.M., Arrigo, K.R., et al. (2000) Rapid and early export of Phaeocystis antarctica

679 blooms in the Ross Sea, Antarctica. *Nature*, 404 (6778): 595–598. doi:10.1038/35007061.

680 Escutia, C., Brinkhuis, H., Klaus, A., et al. (2011) *Expedition 318 summary*.

681 doi:10.2204/iodp.proc.318.101.2011.

682 Farquhar, G.D., O'Leary, M.H. and Berry, J.A. (1982) On the Relationship between Carbon Isotope

683 Discrimination and the Intercellular Carbon dioxide Concentration in Leaves. *Australian Journal of Plant*

684 *Physiology*, 9: 121–137.

685 Fischer, G., Schneider, R., Müller, P.J., et al. (1997) Anthropogenic CO_2 in Southern Ocean surface waters:

686 Evidence from stable organic carbon isotopes. *Terra Nova*, 9 (4): 153–157. doi:10.1046/j.1365-3121.1997.d01-

687 29.x.

688 Francey, R.J., Allison, C.E., Etheridge, D.M., et al. (1999) A 1000-year high precision record of δ13C in

689 atmospheric CO_2. *Tellus, Series B: Chemical and Physical Meteorology*, 51 (2): 170–193.

690 Frignani, M., Giglio, F., Langone, L., Ravaioli, M. & Mangini, A. 1998. Late Pleistocene- Holocene

691 sedimentary fluxes of organic carbon and biogenic silica in the northwestern Ross Sea, Antarctica. *Annals of*

692 *Glaciology*, **27**, 697–703.

693

694 Gibson, J.A.E., Trull, T., Nichols, P.D., et al. (1999) Sedimentation of 13 C-rich organic matter from Antarctic

695 sea-ice algae: A potential indicator of past sea-ice extent. *Geology*, 27 (4): 331–334. doi:10.1130/0091-

696 7613(1999)027<0331:SOCROM>2.3.CO;2.

697 Gilchrist, H. (2018) *A high-resolution record of sea ice, glacial and biological dynamics from an Antarctic*

698 *coast environment*. University of Birmingham.

699 Haddad, R.I., Martens, C.S. and Farrington, J.W. (1992) Quantifying early diagenesis of fatty acids in a rapidly

700 accumulating coastal marine sediment. *Organic Geochemistry*, 19 (1–3): 205–216. doi:10.1016/0146-

701 6380(92)90037-X.

702 Henley, S.F., Annett, A.L., Ganeshram, R.S., et al. (2012) Factors influencing the stable carbon isotopic

703 composition of suspended and sinking organic matter in the coastal Antarctic sea ice environment.

704 *Biogeosciences*, 9 (3): 1137–1157. doi:10.5194/bg-9-1137-2012.

705 Johns, L. et al. (1999) 'Identification of a C25 highly branched isoprenoid (HBI) diene in Antarctic sediments,

706 Antarctic sea-ice diatoms and cultured diatoms', *Organic Geochemistry*, 30(11), pp. 1471–1475. doi:

707 10.1016/S0146-6380(99)00112-6.

708   Jónasdóttir, S. H. (2019) Fatty Acid Profiles and Production in Marine Phytoplankton. Marine Drugs 17, 151.

709   Keeling, C.D., Piper, S.C., Bacastow, R.B., et al. (2005) "Atmospheric CO2 and 13CO2 Exchange with the

710   Terrestrial Biosphere and Oceans from 1978 to 2000: Observations and Carbon Cycle Implications." In A

711   History of Atmospheric CO2 and Its Effects on Plants, Animals, and Ecosystems. doi:10.1007/0-387-27048-

712   5_5.

713   Kopczynska, E.E., Goeyens, L., Semeneh, M., et al. (1995) Phytoplankton Composition and Cell Carbon

714   Distribution in Prydz Bay, Antarctica - Relation To Organic Particulate Matter and Its Delta-C-13 Values.

715   *Journal of Plankton Research*, 17 (4): 685–707. doi:10.1093/plankt/17.4.685.

716   Leblond, J.D. and Chapman, P.J. (2000) LIPID CLASS DISTRIBUTION OF HIGHLY UNSATURATED

717   LONG CHAIN FATTY ACIDS IN MARINE DINOFLAGELLATES. *Journal of Phycology*, 36: 1103–1108.

718   MacFarling Meure, C., Etheridge, D., Trudinger, C., et al. (2006) Law Dome CO2, CH4 and N2O ice core

719   records extended to 2000 years BP. *Geophysical Research Letters*, 33 (14): 1–4. doi:10.1029/2006GL026152.

720   Mackensen, A. (2001) Oxygen and carbon stable isotope tracers of Weddell sea water masses: New data and

721   some paleoceanographic implications. *Deep-Sea Research Part I: Oceanographic Research Papers*, 48 (6):

722   1401–1422. doi:10.1016/S0967-0637(00)00093-5.

723   Massé, G., Belt, S.T., Crosta, X., et al. (2011) Highly branched isoprenoids as proxies for variable sea ice

724   conditions in the Southern Ocean. *Antarctic Science*, 23 (5): 487–498. doi:10.1017/S0954102011000381.

725   Matsuda, H. (1978) Early diagenesis of fatty acids in lacustrine sediments-III. Changes in fatty acid composition

726   in the sediments from a brackish water lake. *Geochimica et Cosmochimica Acta*, 42: 1027–1034.

727   Matsuda, H. and Koyama, T. (1977) Early diagenesis of fatty acids in lacustrine sediments-I. Identification and

728   distribution of fatty acids in recent sediment from a freshwater lake. *Geochimica et Cosmochimica Acta*, 41 (6):

729   777–783. doi:10.1016/0016-7037(77)90048-5.

730   Moisan, T.A. and Mitchell, B.G. (1999) Photophysiological acclimation of Phaeocystis antarctica Karsten under

731   light limitation. *Limnology and Oceanography*, 44 (2): 247–258. doi:10.4319/lo.1999.44.2.0247.

732   Pancost, R.D. and Boot, C.S. (2004) The palaeoclimatic utility of terrestrial biomarkers in marine sediments.

733   *Marine Chemistry*, 92 (1–4 SPEC. ISS.): 239–261. doi:10.1016/j.marchem.2004.06.029.

734   Popp, B. N. et al. (1999) 'Controls on the carbon isotopic composition of Southern Ocean phytoplankton',

735   Global Biogeochemical Cycles, 13(4), pp. 827–843. doi: 10.1029/1999GB900041.

736   Poulton, A.J., Mark Moore, C., Seeyave, S., et al. (2007) Phytoplankton community composition around the

737   Crozet Plateau, with emphasis on diatoms and Phaeocystis. *Deep-Sea Research Part II: Topical Studies in*

738   *Oceanography*, 54 (18–20): 2085–2105. doi:10.1016/j.dsr2.2007.06.005.

739   Rau, G.H., Takahashi, T. and Des Marais, D.J. (1989) Latitudinal variations in plankton δ^{13}C: Implications for

740   CO_2 and productivity in past oceans. *Nature*, 341 (6242): 516–518.

741   Riaux-gobin, C., Dieckmann, G.S., Poulin, M., et al. (2013) *Environmental conditions , particle flux and*

742 *sympagic microalgal succession in spring before the sea-ice break-up in Adé lie Land , East Antarctica*

743 *Environmental conditions , particle flux and sympagic microalgal ´ lie Land , succession in spring before t.,*

744 (May 2014): 0–25. doi:10.3402/polar.v32i0.19675.

745 Riaux-Gobin, C., Dieckmann, G.S., Poulin, M., et al. (2013) Environmental conditions, particle flux and

746 sympagic microalgal succession in spring before the sea-ice break-up in Adélie Land, East Antarctica. *Polar*

747 *Research*, 32 (SUPPL.): 0–25. doi:10.3402/polar.v32i0.19675.

748 Riaux-Gobin, C., Poulin, M., Dieckmann, G., et al. (2011) Spring phytoplankton onset after the ice break-up and

749 sea-ice signature (Ad??lie Land, East Antarctica). *Polar Research*, 30 (SUPPL.1).

750 doi:10.3402/polar.v30i0.5910.

751 Roden, N.P., Shadwick, E.H., Tilbrook, B., et al. (2013) Annual cycle of carbonate chemistry and decadal

752 change in coastal Prydz Bay, East Antarctica. *Marine Chemistry*, 155: 135–147.

753 doi:10.1016/j.marchem.2013.06.006.

754 Salminen, T.A., Eklund, D.M., Joly, V., et al. (2018) Deciphering the evolution and development of the cuticle

755 by studying lipid transfer proteins in mosses and liverworts. *Plants*, 7 (1). doi:10.3390/plants7010006.

756 Sambrotto, R.N., Matsuda, A., Vaillancourt, R., et al. (2003) Summer plankton production and nutrient

757 consumption patterns in the Mertz Glacier Region of East Antarctica. *Deep-Sea Research Part II: Topical*

758 *Studies in Oceanography*, 50 (8–9): 1393–1414. doi:10.1016/S0967-0645(03)00076-6.

759 Shadwick, E.H., Tilbrook, B. and Williams, G.D. (2014) Carbonate chemistry in the Mertz Polynya (East

760 Antarctica): Biological and physical modification of dense water outflows and the export of anthropogenic CO2.

761 *Journal of Geophysical Research: Oceans*, 119 (1): 1–14. doi:10.1002/2013JC009286.

762 Shevenell, A.E. and Kennett, J.P. (2002) *Antarctic Holocene climate change : A benthic foraminiferal stable*

763 *isotope record from Palmer Deep.*, 17 (2).

764 Sigman, D. and Boyle, E. (2000) Glacial/interglacial variations in atmospheric carbon dioxide. *Nature*, 407

765 (6806): 859–869.

766 Sinninghe Damsté, J.S., Rijpstra, W.I.C., Coolen, M.J.L., et al. (2007) Rapid sulfurisation of highly branched

767 isoprenoid (HBI) alkenes in sulfidic Holocene sediments from Ellis Fjord, Antarctica. *Organic Geochemistry*,

768 38 (1): 128–139. doi:10.1016/j.orggeochem.2006.08.003.

769 Skerratt, J.H., Davidson, A.D., Nichols, P.D., et al. (1998) Effect of UV-B on lipid content of three antarctic

770 marine phytoplankton. *Phytochemistry*, 49 (4): 999–1007. doi:10.1016/S0031-9422(97)01068-6.

771 Smik, L., Belt, S.T., Lieser, J.L., et al. (2016) Distributions of highly branched isoprenoid alkenes and other

772 algal lipids in surface waters from East Antarctica: Further insights for biomarker-based paleo sea-ice

773 reconstruction. *Organic Geochemistry*, 95: 71–80. doi:10.1016/j.orggeochem.2016.02.011.

774 Sun, M.Y., Zou, L., Dai, J., et al. (2004) Molecular carbon isotopic fractionation of algal lipids during

775 decomposition in natural oxic and anoxic seawaters. *Organic Geochemistry*, 35 (8): 895–908.

776 doi:10.1016/j.orggeochem.2004.04.001.

777   Sweeney, C. (2003) "The annual cycle of surface water CO2 And O2 in the Ross Sea: A model for gas
778   exchange on the continental shelves of Antarctica." In *Antarctic Research Series Vol 78*. doi:10.1029/078ars19.

779   Takahashi, T., Sutherland, S.C., Wanninkhof, R., et al. (2009) Climatological mean and decadal change in
780   surface ocean pCO2, and net sea-air CO2 flux over the global oceans. *Deep-Sea Research Part II: Topical*
781   *Studies in Oceanography*, 56 (8–10): 554–577. doi:10.1016/j.dsr2.2008.12.009.

782   Tortell, P.D., Guéguen, C., Long, M.C., et al. (2011) Spatial variability and temporal dynamics of surface water
783   pCO2, δO2/Ar and dimethylsulfide in the Ross Sea, Antarctica. *Deep-Sea Research Part I: Oceanographic*
784   *Research Papers*, 58 (3): 241–259. doi:10.1016/j.dsr.2010.12.006.

785   Tréguer, P., Bowler, C., Moriceau, B., et al. (2017) Influence of diatom diversity on the ocean biological carbon
786   pump. Nature Geoscience. doi:10.1038/s41561-017-0028-x.

787   Vaillancourt, R.D., Sambrotto, R.N., Green, S., et al. (2003) Phytoplankton biomass and photosynthetic
788   competency in the summertime Mertz Glacier region of East Antarctica. *Deep-Sea Research Part II: Topical*
789   *Studies in Oceanography*, 50 (8–9): 1415–1440. doi:10.1016/S0967-0645(03)00077-8.

790   Villinski, J.C., Hayes, J.M., Brassell, S.C., et al. (2008) Sedimentary sterols as biogeochemical indicators in the
791   Southern Ocean. *Organic Geochemistry*, 39 (5): 567–588. doi:10.1016/j.orggeochem.2008.01.009.

792   Wakeham, S.G., Lee, C., Farrington, J.W., et al. (1984) Biogeochemistry of particulate organic matter in the
793   oceans: results from sediment trap experiments. *Deep Sea Research Part A, Oceanographic Research Papers*,
794   31 (5): 509–528. doi:10.1016/0198-0149(84)90099-2.

795   Williams, G.D. and Bindoff, N.L. (2003) Wintertime oceanography of the Adélie Depression. *Deep-Sea*
796   *Research Part II: Topical Studies in Oceanography*, 50 (8–9): 1373–1392. doi:10.1016/S0967-0645(03)00074-
797   2.

798   Wilson, D.L., Smith, W.O. and Nelson, David, M. (1986) *Phytoplankton bloom dynamics of the western Ross*
799   *Sea ice edge - I. Primary productivity and species-specific production.*, 33 (10): 1375–1387.

800   Wong, W.W. and Sackett, W.M. (1978) Fractionation of stable carbon isotopes by marine phytoplankton.
801   *Geochimica et Cosmochimica Acta*, 42 (12): 1809–1815. doi:10.1016/0016-7037(78)90236-3.

802   Zhang, R., Zheng, M., Chen, M., et al. (2014) An isotopic perspective on the correlation of surface ocean carbon
803   dynamics and sea ice melting in Prydz Bay (Antarctica) during austral summer. *Deep-Sea Research Part I:*
804   *Oceanographic Research Papers*, 83: 24–33. doi:10.1016/j.dsr.2013.08.006.

805

806
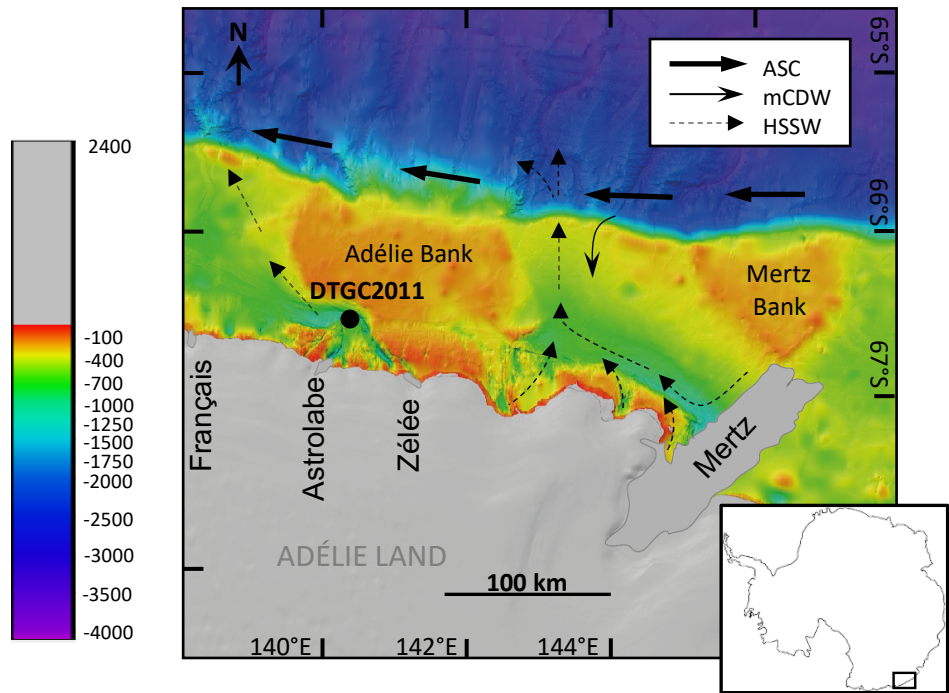
Figure 1: Location of Site DTGC2011 on bathymetric map of the Adélie Land region (modified from Beaman et al., 2011), indicating positions of the main glaciers (prior to Mertz Glacier Tongue collapse in 2010) and pathways of the main water masses affecting the region: Antarctic Slope Current (ASC), Modified Circumpolar Deep Water (mCDW) and High Shelf Salinity Water (HSSW) (Williams and Bindoff, 2003).

807

808

809

810

811

812

813

814

815

816

817

818

819

820

821

822

823

824

825

826

827
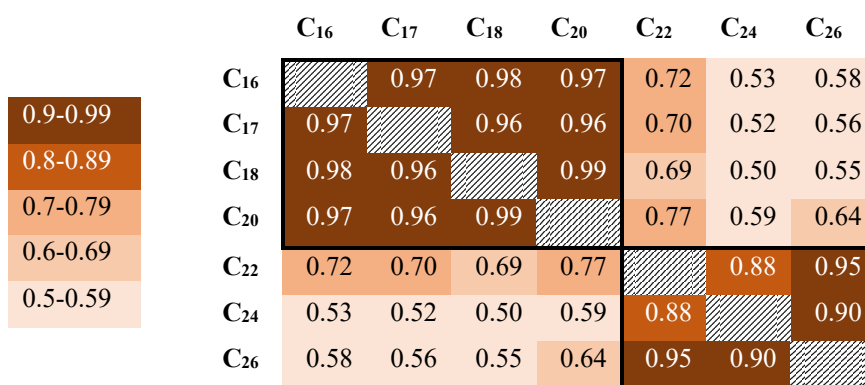
Figure 3: R^2 values for fatty acid concentrations throughout core DTGC2011. Values are colour coded according to the key on the left. Black border denotes correlations within each group.

837

845
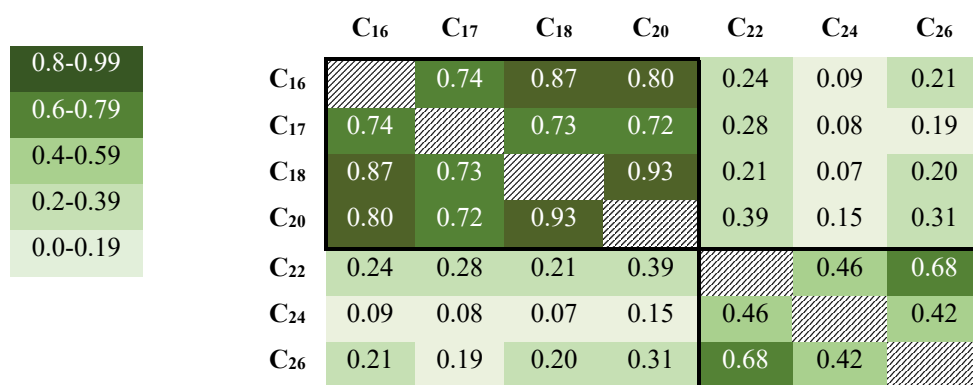
Figure 4: R^2 values for fatty acid concentrations in core DTGC2011 below 25 cm only. Values are colour coded according to the key on the left. Black border denotes correlations within each group.
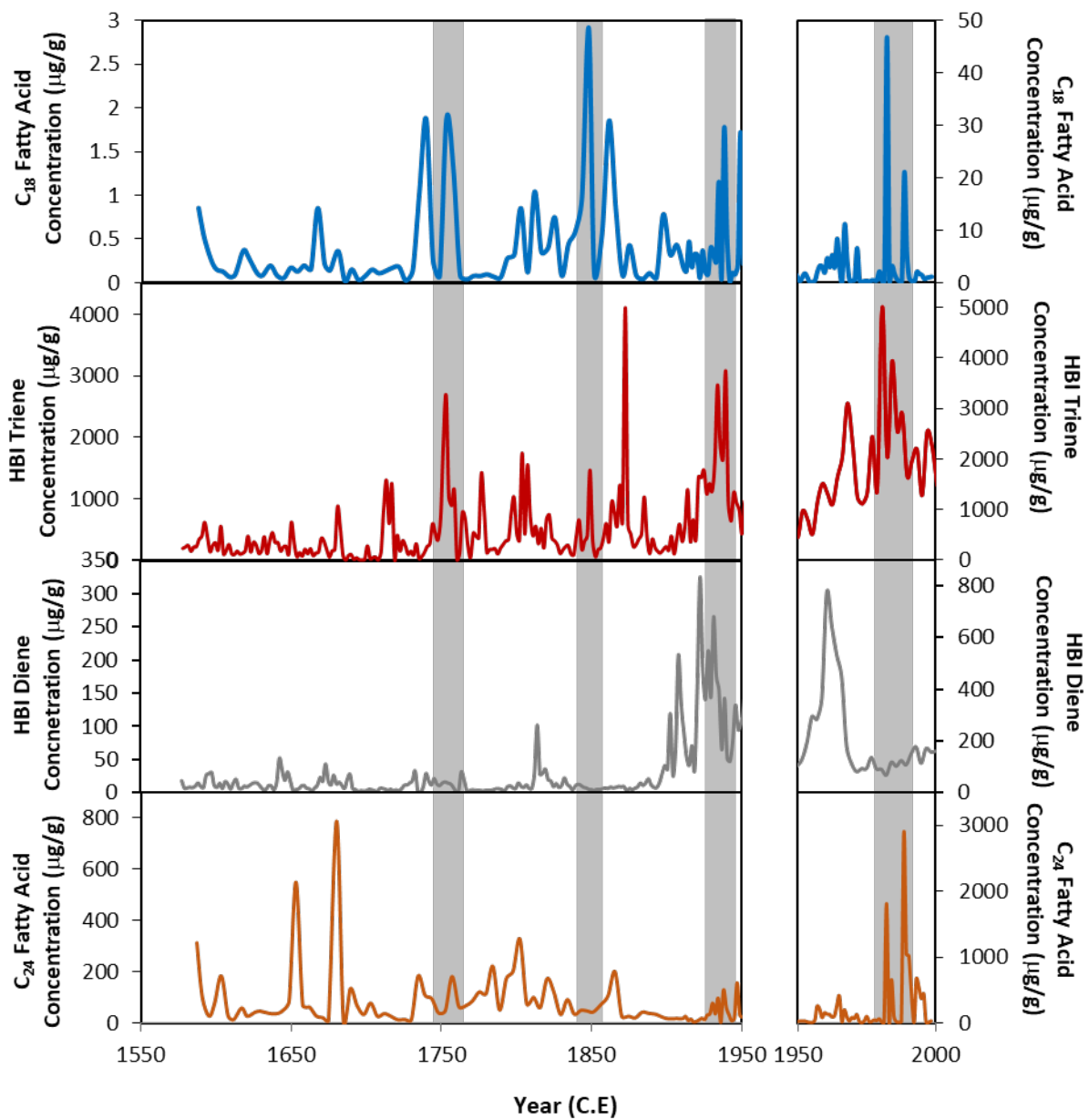
Figure 5: Concentrations of the C$_{18}$ fatty acid (blue), the HBI triene (red), HBI diene (grey) (Campagne, 2015), C$_{24}$ fatty acid (orange) from core DTGC2011. The left-hand panels show 1550 to 1950 C.E. and the right hand panels show 1950 to 2000 C.E., plotted on different y-axes due to the elevated concentrations in the top part of the core. Grey vertical bands highlight coincident peaks in C$_{18}$ fatty acid and HBI triene records.

847
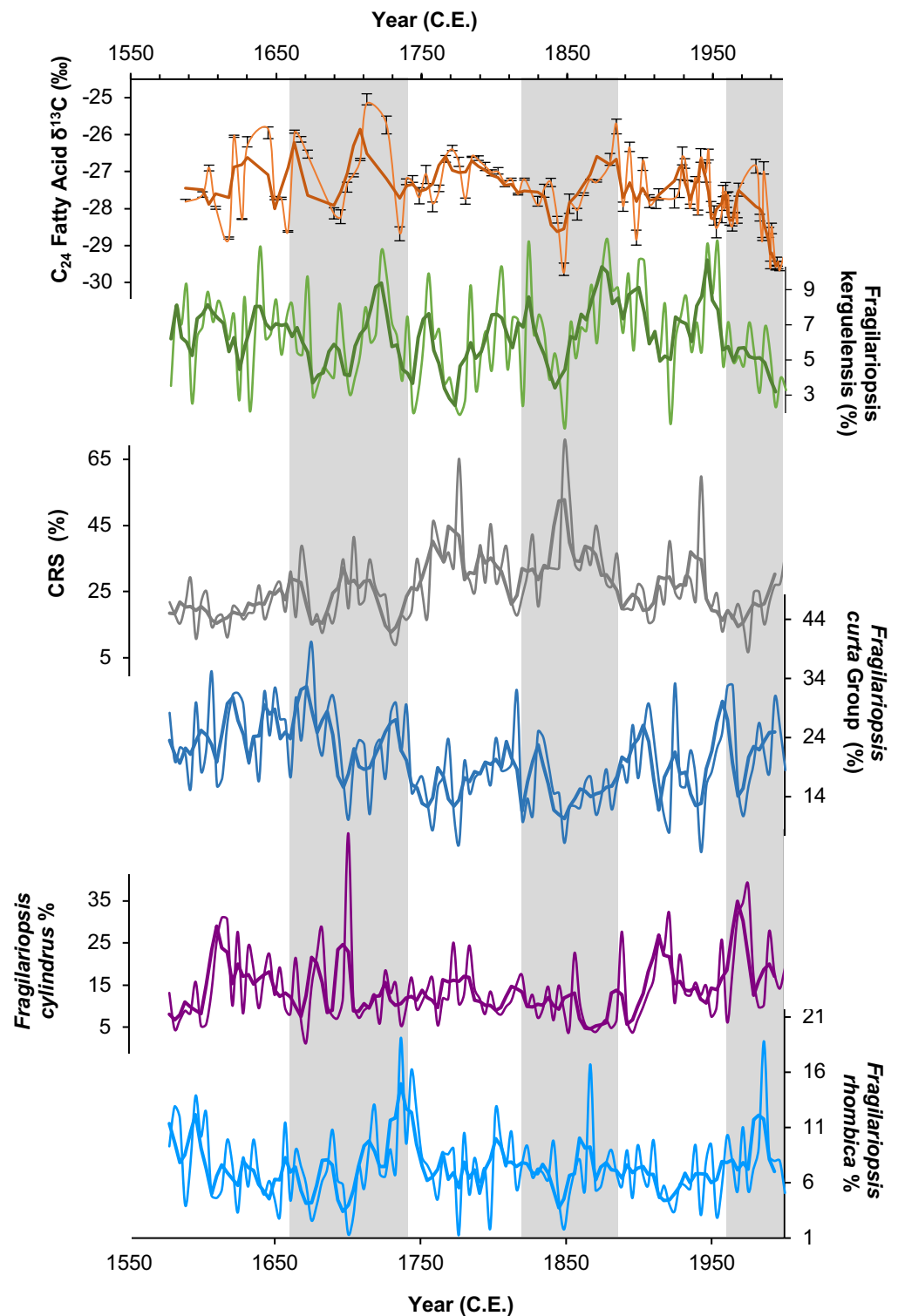
Figure 6: δ¹³C values of the C₂₄ fatty acid (orange) and relative abundances (%) of the open water diatom *Fragilariopsis kerguelensis* **(green). Also shown are relative abundances of the four most abundant diatom groups in DTGC2011.** *Chaetoceros* **resting spores (CRS; grey line),** *Fragilariopsis curta* **group (dark blue line),** *Fragilariopsis cylindrus* **(purple line) and** *Fragilariopsis rhombica* **(light blue line). Thick line represents 3-point moving average for each. Grey vertical bands highlight periods where C₂₄ fatty acid δ¹³C is in phase with** *F. kerguelensis.*
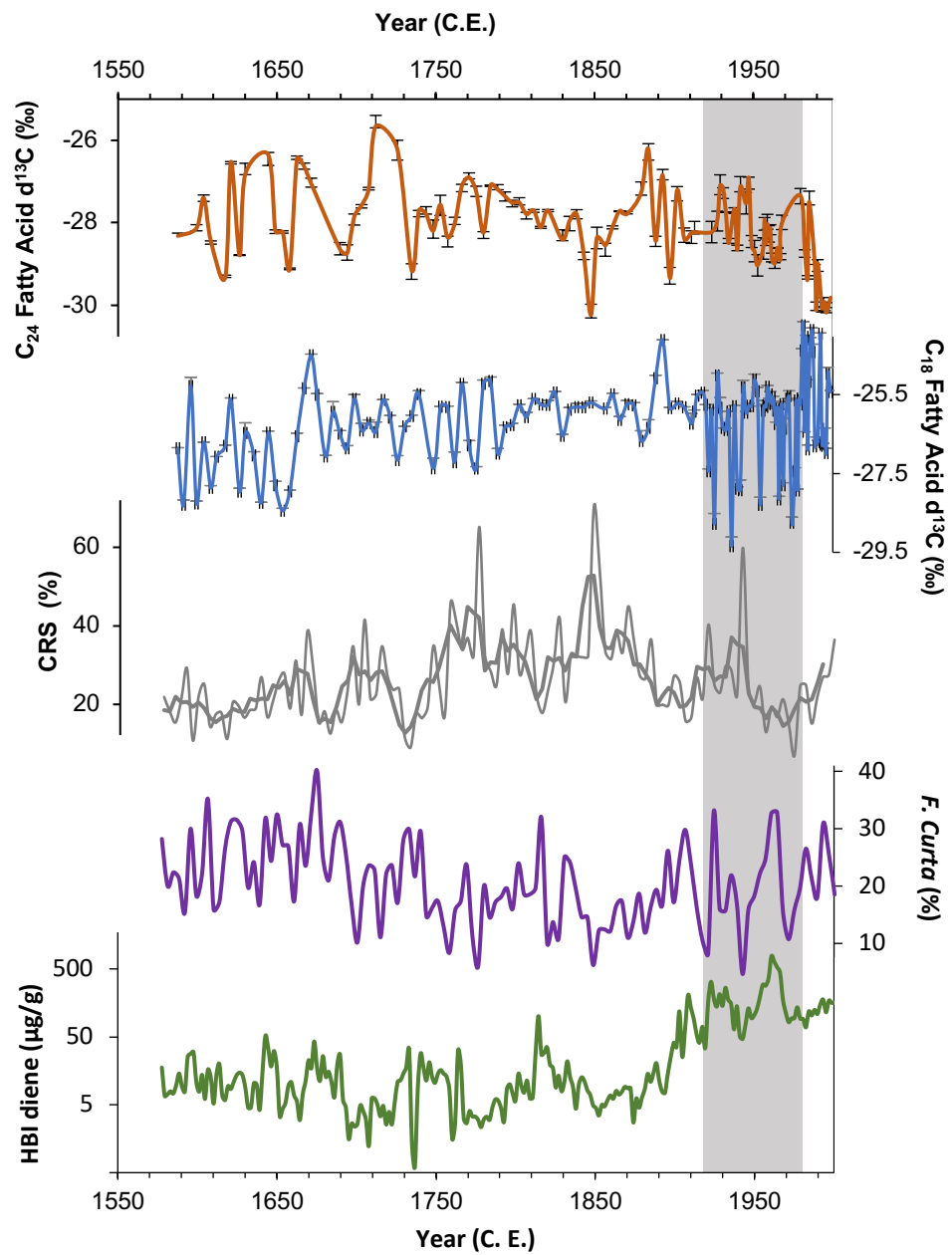
Figure 7: δ¹³C of the C$_{24}$ (orange) and C$_{18}$ (blue) fatty acid, HBI diene concentrations (green; plotted on a log scale) and relative abundances of *Fragilariopsis curta* plus *Fragilariopsis cylindrus* (purple). Latter two records reflect sea ice concentrations. Grey vertical band highlights period where low C$_{18}$ δ¹³C overlaps with elevated HBI diene concentrations.